AN EXPERIMENTAL INVESTIGATION OF NUCLEATE BOILING IN THIN LIQUID FILMS

Almon Duncan Rivers

NAVAL POSTGRADUATE SCHOOL
Monterey, California

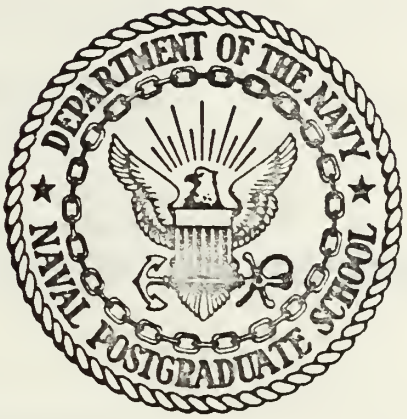

THESIS

AN EXPERIMENTAL INVESTIGATION
OF
NUCLEATE BOILING IN THIN LIQUID FILMS

by

Almon Duncan Rivers

June 1974

Thesis Advisor: Paul J. Marto

Approved for public release; distribution unlimited.

REPORT DOCUMENTATION PAGE

READ INSTRUCTIONS BEFORE COMPLETING FORM

1. REPORT NUMBER

2. GOVT ACCESSION NO.

3. RECIPIENT'S CATALOG NUMBER

4. TITLE (and Subtitle)
An Experimental Investigation of Nucleate Boiling in Thin Liquid Films

5. TYPE OF REPORT & PERIOD COVERED
Master's Thesis; June 1974

6. PERFORMING ORG. REPORT NUMBER

7. AUTHOR(s)
Almon D. Rivers

8. CONTRACT OR GRANT NUMBER(s)

9. PERFORMING ORGANIZATION NAME AND ADDRESS
Naval Postgraduate School
Monterey, California 93940

10. PROGRAM ELEMENT, PROJECT, TASK AREA & WORK UNIT NUMBERS

11. CONTROLLING OFFICE NAME AND ADDRESS
Naval Postgraduate School
Monterey, California 93940

12. REPORT DATE
June 1974

13. NUMBER OF PAGES
61

14. MONITORING AGENCY NAME & ADDRESS(if different from Controlling Office)

15. SECURITY CLASS. (of this report)
Unclassified

15a. DECLASSIFICATION/DOWNGRADING SCHEDULE

16. DISTRIBUTION STATEMENT (of this Report)
Approved for public release; distribution unlimited.

17. DISTRIBUTION STATEMENT (of the abstract entered in Block 20, if different from Report)

18. SUPPLEMENTARY NOTES

19. KEY WORDS (Continue on reverse side if necessary and identify by block number)
Nucleate Boiling
Thin Liquid Films
Cholesteric Liquid Crystals

20. ABSTRACT (Continue on reverse side if necessary and identify by block number)
Experimental data was taken to determine the heat transfer coefficient during boiling of Freon 113 in thin liquid films from a horizontal, rectangular foil .025 mm thick. Heat flux was held constant at 8, 12, 16 and 32 thousand watts/m^2 as liquid level was lowered from 18mm to 0.2mm below which dryout usually occurred. Quantitative temperature data was taken with copper-constantan thermocouples. In addition, surface temperature of the foil was qualitatively mapped with Cholesteric Liquid Crystals. This

20.
mapping was recorded and is presented by color photographs. There is an increase in heat transfer coefficient as liquid level is lowered below 2.0 mm for Freon 113. This increase is more noticeable at the lower heat fluxes. Liquid Crystals are a practical means of mapping the nucleation sites on the surface of a thin foil boiling test section. The heating surface under the bubbles forming on the surface is cooler than under the undisturbed liquid. As heat flux increases the number of active nucleation sites also increases. The wetted-unwetted boundary at dryout is cooler than either the wetted or unwetted surface.

An Experimental Investigation of Nucleate Boiling in Thin Liquid Films

by

Almon Duncan Rivers
Lieutenant, United States Navy
B.S., United States Naval Academy, 1967

Submitted in partial fulfillment of the
requirements for the degree of

MASTER OF SCIENCE IN MECHANICAL ENGINEERING

from the

NAVAL POSTGRADUATE SCHOOL
June 1974

ABSTRACT

Experimental data was taken to determine the heat transfer coefficient during boiling of Freon 113 in thin liquid films from a horizontal, rectangular foil .025 mm thick. Heat flux was held constant at 8, 12, 16 and 32 thousand watts/m^2 as liquid level was lowered from 18mm to 0.2mm below which dryout usually occurred. Quantitative temperature data was taken with copper-constantan thermocouples. In addition, surface temperature of the foil was qualitatively mapped with Cholesteric Liquid Crystals. This mapping was recorded and is presented by color photographs.

There is an increase in heat transfer coefficient as liquid level is lowered below 2.0 mm for Freon 113. This increase is more noticeable at the lower heat fluxes. Liquid Crystals are a practical means of mapping the nucleation sites on the surface of a thin foil boiling test section. The heating surface under the bubbles forming on the surface is cooler than under the undisturbed liquid. As heat flux increases the number of active nucleation sites also increases. The wetted-unwetted boundary at dryout is cooler than either the wetted or unwetted surface.

TABLE OF CONTENTS

LIST OF FIGURES

LIST OF SYMBOLS

SYMBOL	MEANING
TC	Thermocouple
k	Thermal conductivity
S	Inline resistor voltage
F	Test section terminal voltage
Rs	Inline resistance
q''	Heat flux
PWR	Test section power
A	Test surface area
L'	Test section length
L	Heat loss through glass block
t	Thickness of glass block
Tw	Test surface temperature
T3	Glass bottom temperature
Ts	Fluid saturation temperature
A-PWR	Auxiliary heater power
V	Voltage from auxiliary power supply
a	Current from auxiliary power supply
h	Heat transfer coefficient
H	Liquid level

ACKNOWLEDGEMENTS

I would like to express my deepest gratitude to the following people for their contributions to this effort. To Dr. Paul Marto for his invaluable guidance and encouragement. To my wife Sue for her extreme tolerance and assistance with the test sections and drawings. To George Bixler and Tom Christian who spent many hours in the construction and repair of the test apparatus. And to Frank and Mary Galietta who so graciously housed us during the final writing of this thesis.

I. INTRODUCTION

A. BACKGROUND

Several motivations for the study of nucleate boiling at low liquid levels were given by MacKenzie [1] with special emphasis on the applicability of this phenomenon to heat pipes and their Naval uses. A greater knowledge of this method of heat transfer might also contribute toward increasing the efficiency of our nuclear power generating plants which utilize liquid flowing through narrow channels to remove the heat generated by the nuclear fuel. The capacity of this liquid to remove heat controls the temperature of the channel walls and thus the amount of heat that may be generated in them. If the liquid were allowed to transfer heat by operating in the region of nucleate boiling the resulting lower wall temperatures in the channel would allow for the generation of more heat per unit volume of the reactor core.

Nishikawa, et al. [2] noted an increase in the heat transfer coefficient as liquid level was lowered from 50 to 1 mm. and studied the effects of various fluids on this phenomenon. Among their several observations were the following:

1. Below 30mm in water, bubbles climb straight up rather than in the circular convection paths common to pool boiling.

2. As heat flux increases the number of active nucleation sites also increases.

3. Large vapor domes were formed at low liquid levels but do not play an important role in the boiling heat transfer since their influence would tend to decrease the heat transfer coefficient which was observed to increase.

4. The slope of the boiling curve at low liquid levels differs from that observed during pool boiling.

5. The lower the heat flux the more remarkable the effect of liquid level on the heat transfer coefficient.

6. The number of nucleation sites increases as the liquid level is lowered.

MacKenzie [1] noted this increase in heat transfer coefficient at liquid levels below 5.08mm (.2 inches) in distilled water and ethyl-alcohol and studied the effect of surface condition on this phenomenon. Review of MacKenzie's data also reveals that the increase in h is more pronounced at lower heat fluxes.

Grigor'ev and Dudkevich [3] noted this same trend of greater heat transfer in thin liquid films while studying boiling in cryogenic liquids and studied the effect of different surface materials on the boiling phenomena with specific emphasis on critical heat flux, i.e., the heat flux at which dryout occurs.

Raad and Myers [4] studied the use of liquid crystals in determining the number of nucleation sites during pool boiling. They experienced some difficulty with convection currents cooling their test section and

distorting the nucleation site data. They were thus unable to present any quantitative results.

As explained by Rivers and Field [5] the cholesteric liquid crystals experience color changes from black to red to green to blue as they are heated through their range of event temperatures. They change in the opposite sequence as they are cooled. When heated well above their event temperature the blue color deepens to a dark blue or black which is not readily discernable from the black seen below the event temperature.

Rivers and Field [5] used the liquid crystals to map the surface temperature of a heated cylinder in forced and free convection. Sheppard [6] used the crystals to map the surface temperature of various electronic circuit boards. Liquid crystals were also used by Roger D. Maple [7] to map the surface temperature of sonar transducers. Several other studies have been made at the Naval Postgraduate School on the use of liquid crystals in temperature mapping.

B. THESIS OBJECTIVE

The objective of this thesis was twofold, first to reproduce the effect of liquid level on heat transfer coefficient seen by Nishikawa and MacKenzie, and second to use temperature sensitive liquid crystals to correlate this increase in heat transfer coefficient with the increase in nucleation sites as level is lowered as observed by Nishikawa.

II. EXPERIMENTAL DESIGN

A. FACTORS CONSIDERED

The overall design of the boiling apparatus used in this study was greatly influenced by the requirement to allow boiling from the test section while mapping with liquid crystals the temperature variations on the test surface caused by the boiling. It was also required that the system maintain a nearly constant mass of boiling fluid to insure a constant liquid level while readings were being taken. The bulk fluid in the system was to be maintained at saturation conditions throughout the testing. The following parameters were to be determined as accurately as possible:

1. Test section wall temperature
2. Bulk fluid temperature
3. Vapor temperature
4. Liquid level relative to the boiling surface
5. Power required to maintain system at saturation conditions
6. Boiling heat flux from test surface

B. DESCRIPTION OF COMPONENTS

Figure 1 shows schematically the set up of the test apparatus for the major testing and identifies all major components. The use of liquid crystals to map nucleation sites dictated the use of a thin metal

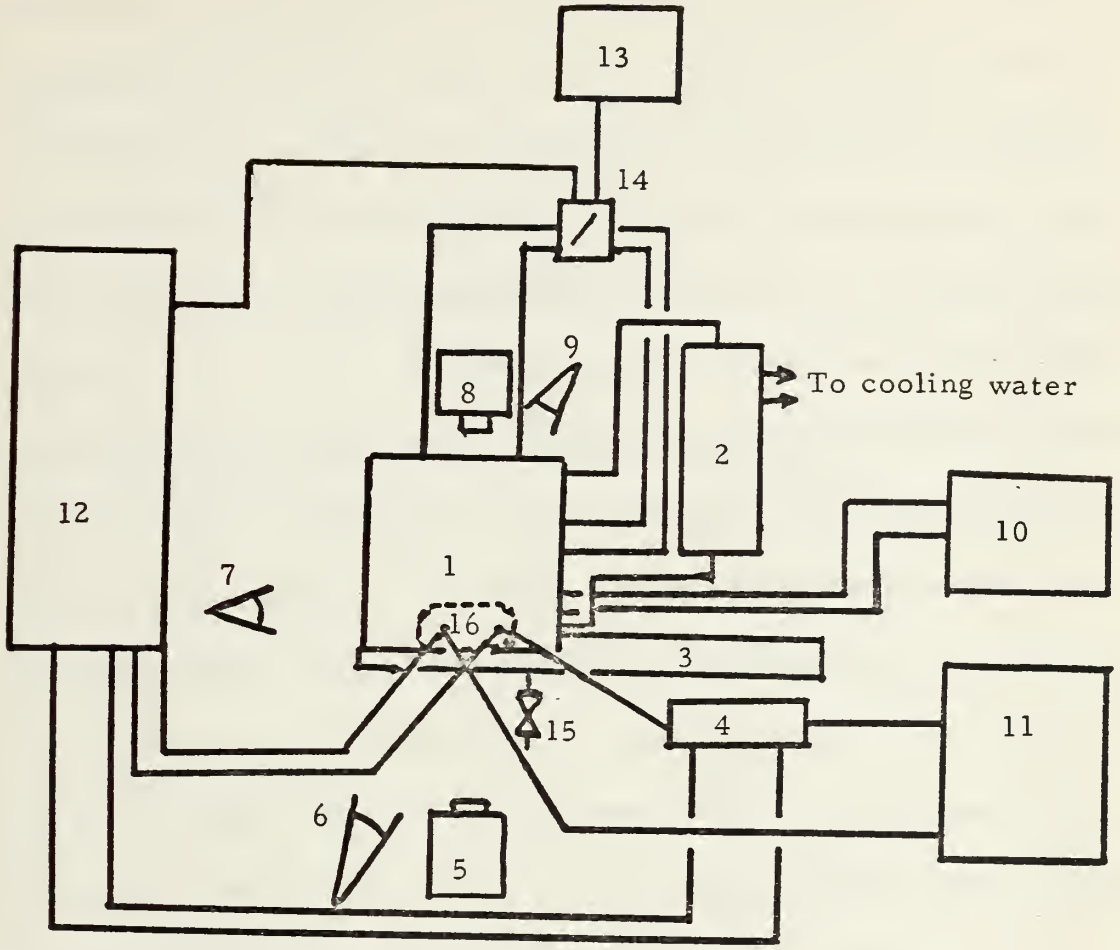

Figure 1.
Schematic of test apparatus set up for final testing

KEY:
1. Test vessel
2. Condenser
3. Vessel support assembly
4. Calibrated inline resistor
5. Rolleiflex camera for photographing crystals
6. Color Tran lights
7. Desk light in position to take B&W photos
8. Nikon camera for photographing boiling surface
9. Desk light in position for measuring level
10. Auxiliary power supply
11. Test section power supply
12. Data acquisition system
13. Reference ice bath
14. Thermocouple switch
15. Vessel drain valve
16. Test section power terminals

foil as the test section. The geometry of the foil was based on generating the desired heat fluxes by passing an electric current through the foil with an available power supply. The foil material was determined on the basis of resistivity, temperature coefficient of resistivity, cost and availability. The foil was stretched between two large copper electrodes as shown in Figure 2 with liquid crystals painted on the bottom. The foil was sealed with clear epoxy cement to the large glass block shown in Figure 2 which allowed the crystals to be viewed from the bottom while protecting them from attack by the boiling fluid. This glass block also served to insulate the bottom of the test section. The test section of the foil measured 50.8mm long X 25.4mm wide X .0254mm thick. The glass block measured 50.8 X 25.4 X 25.4mm. The assembly shown in Figure 2 was mounted on adjustable connections to two 6.35mm copper rods that were mounted in insulating blocks through the side of the test vessel.

The test vessel consisted of a cubical box measuring 203.2mm on the inside edges constructed of one-quarter inch brass plate. This vessel, shown in Figure 3 without insulation, was provided with viewing windows on the top, bottom, and front; six thermocouple connection ports; an inlet port and support for the liquid level measuring device; vapor and condensate connection ports for connection to the condenser; insulated power inlet ports for the test section and auxiliary heaters; and a removable left side to allow easy interchange of test sections

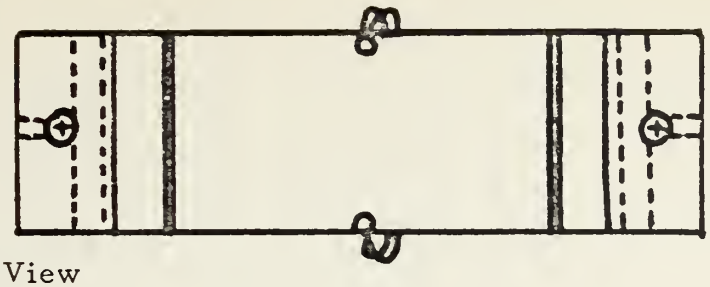

Top View

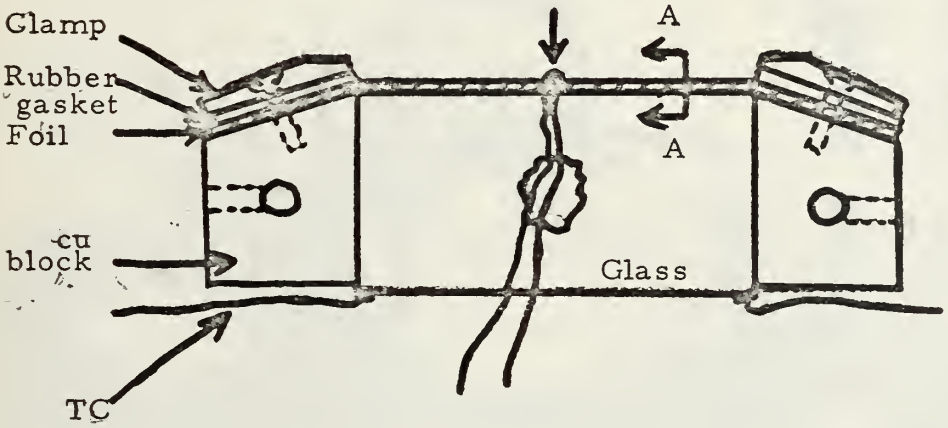

Side View

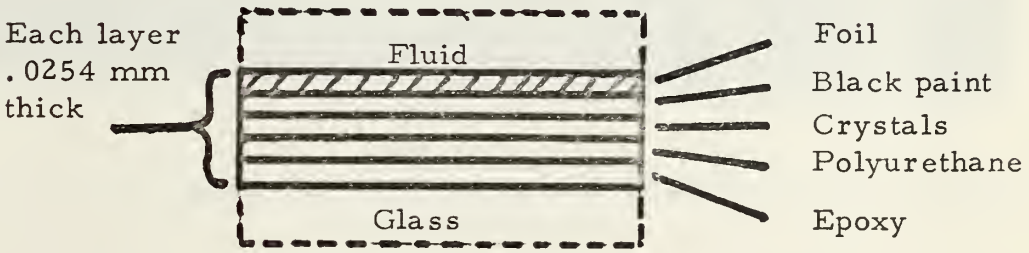

Section AA - Not to scale

Figure 2
Details of Test Section

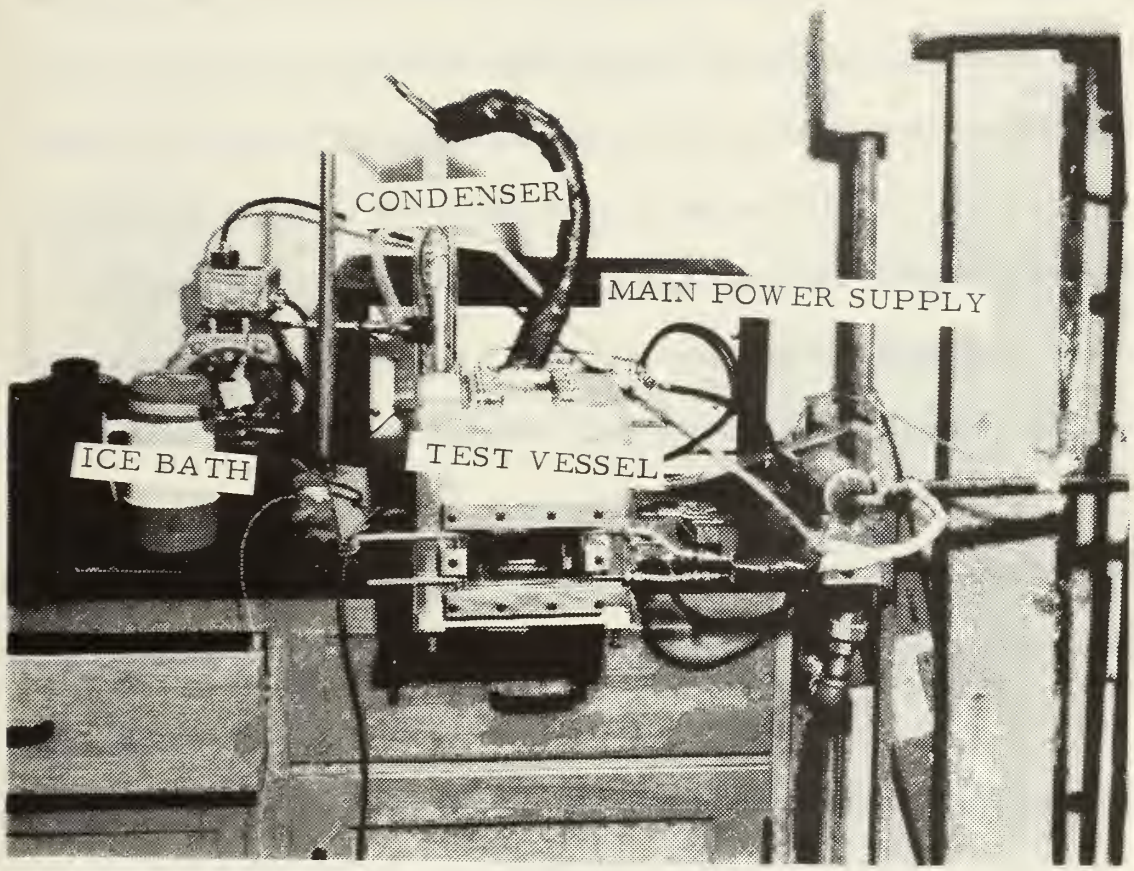

Figure 3.
Front view of test vessel in position
(without insulation)

and instrumentation. The vessel was mounted on a cantilevered support from the work bench. This arrangement provided relatively easy viewing from top, bottom, and front. The support bracket was provided with thumbscrews at the corners for leveling the test section. A drain was also provided on the bottom of the vessel. The entire test vessel was surrounded with thermal insulation to prevent heat losses to ambient. A glass condenser was provided external to the test vessel to return the condensate to the vessel.

A sheathed coil heating element was installed in the liquid portion of the test vessel to heat the fluid and maintain the system at saturation conditions. Power was supplied to this coil from a Lambda Model IK 345A regulated D. C. power supply.

Power was supplied to the test section from a regulated DC power supply with a twelve volt 100 amp capacity. This device was fed from line power through a Powerstat variac.

The liquid crystals used in this study were from the same batch as those used by Rivers and Field [5]. Their calibration data was used to determine which crystal was most appropriate for this study.

C. INSTRUMENTATION

All temperatures were measured with copper constantan thermocouples. The thermocouples for reading vapor, bulk fluid, and glass bottom temperatures were arranged in pairs and read in parallel.

The thermocouples on the test foil were read separately. All thermocouples were referenced to a distilled water ice bath. The thermocouples were attached to a six position switch whose output was read and recorded by the Hewlett-Packard Model 2010C Data Acquisition system.

A calibrated in-line resistor was installed in the power line to the test section as shown in Figure 1. The voltage across this resistor was read and used to determine the current through the test section. The voltage across the test section was read from the power terminals as shown in Figure 1. These voltages were read and recorded by the data acquisition system mentioned above.

The liquid level was measured with a depth micrometer and probe mounted on the top of the test vessel. This instrument with graduations down to .0001 inch was the same device used by MacKenzie [1] modified for mounting on the test vessel described in Section B.

III. EXPERIMENTAL PROCEDURE

A. PREPARATION OF TEST SECTION

The first consideration in preparing the test section was to accurately determine the foil temperature. The foil material was selected to maximize both resistivity and temperature coefficient of resistivity. This requirement was based on a plan to generate a temperature versus resistance curve for the foil. This curve was to be used to determine the foil temperature during operation by measuring the resistance of the foil during boiling. The metals with the most desirable properties were nickel/iron alloys, platinum, and palladium. A study of cost and availability resulted in the selection of palladium and 77% Ni./18% Fe. alloy foils. These foils were mounted on the test sections as shown in Figure 2 without the crystals or sealers and immersed in the Rosemont constant temperature bath. Temperature was raised from room temperature to about 120°C in ten degree increments. At each increment the temperature was allowed to stabilize for 15 minutes and the resistance read and recorded. This procedure resulted in a curve with a large uncertainty band that made it unusable for its intended purpose. In addition, the nickel/iron foil demonstrated a definite aging effect of resistance with temperature. A second calibration run using a one hour wait time was conducted to

verify the above results. This method of temperature measurement was then abandoned.

The second method of foil temperature measurement attempted was the use of intrinsic thermocouples welded to the foil. These thermocouples were welded with the copper elements on one side and the constantan elements on the other side of the foils as shown in Figure 4. These thermocouples were calibrated satisfactorily but their use was prevented by the establishment of cross field potentials when power was applied to the test section.

The final test section was constructed of the nickel/iron material with flattened bead thermocouples welded to each side at approximately the mid point of the test section. These foils were mounted in test jigs as shown in Figure 5 for calibration and application of the crystals. These units and the thermocouples for measurement of vapor, bulk fluid, and glass bottom temperatures were immersed in the Rosemont constant temperature bath. The bath temperature was raised and lowered through a range of temperatures from room temperature to 70°C and the output voltage read and recorded by the data acquisition system with the switch hookup to be used in the actual data runs. This data was plotted as millivolts indicated versus the difference between millivolts recorded and millivolt equivalent of the standard temperature read on the platinum resistance thermometer. This curve resulted in a correction factor of .006 millivolts which was added to the recorded millivolt readings prior to converting to temperature.

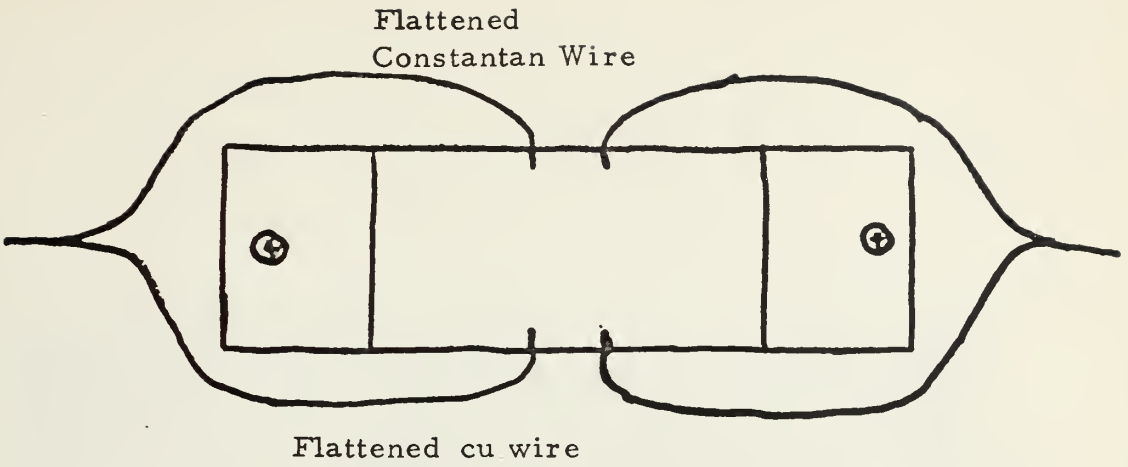

Figure 4.
Test Section Schematic Showing Installation of
Intrinsic Thermocouples

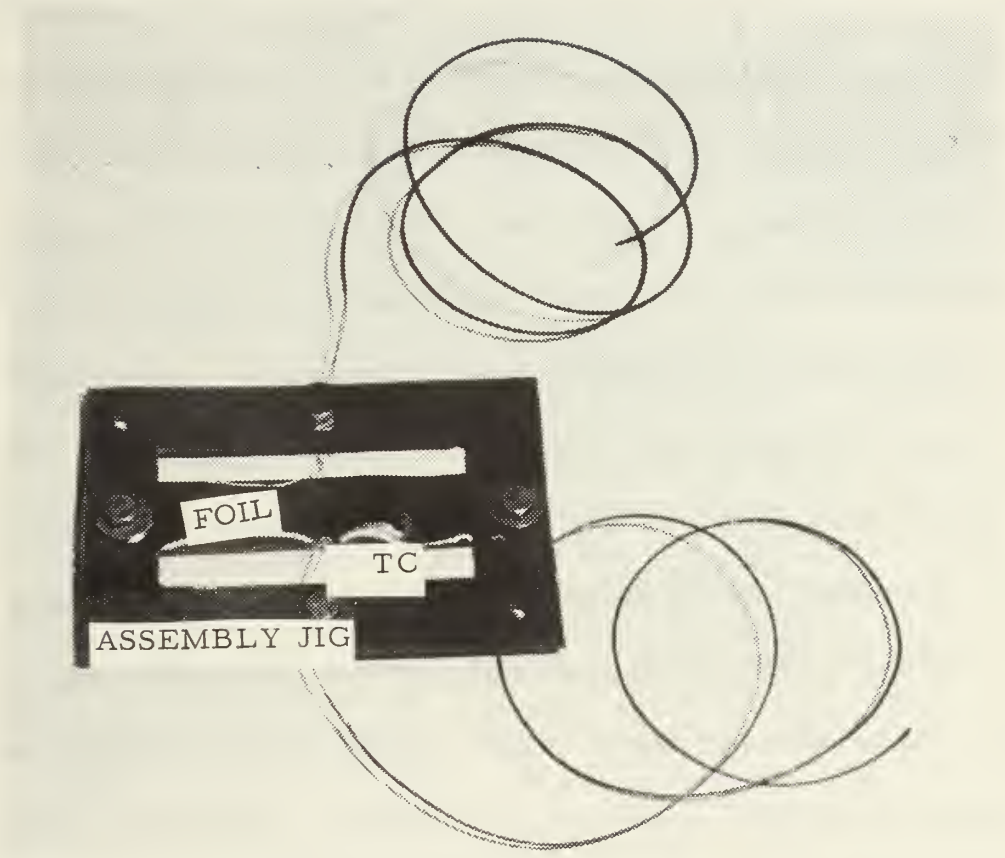

Figure 5.
Test foil mounted for calibration

The data presented in this report was collected in two separate groups which will be referred to as Group A and Group B based on the chronological order in which they were obtained.

The assembly of the test section was begun by attaching the copper electrode blocks to the glass blocks with epoxy cement which was allowed to set up overnight. The foil was then prepared by painting the bottom with two coats of Testor's flat black paint followed by three coats of liquid crystals mentioned in Section II. For the Group A testing NCR R-59 and R-56 crystals were used and for the Group B the NCR R-59 crystal was used. The crystals were sealed with Rez Polyurethane. Each coat of paint, crystals, and polyurethane was dried under a heat lamp. The foil was then attached to the glass and copper block assembly by the application of quick setting Duro Epoxy cement to both foil and glass and clamping in position with parallel clamps. Extreme care was necessary during this procedure to avoid breaking the thermocouples. This cement was allowed to cure overnight to establish a complete seal and bond. The thermocouple wires were then bonded to the sides of the glass block with the same epoxy to prevent damage to the thermocouples during future handling.

All thermocouple wires were inserted in 3.175 mm brass or stainless tubes and sealed with epoxy. These tubes were then installed through the walls of the test vessel using the ports provided and sealed with compressible rubber tube fittings. The test section was then

clamped in place as shown in Figure 6 with adjustable clamps. The tubes containing the thermocouples for measuring the vapor and bulk fluid temperatures were installed through the top of the vessel and bent 90° to allow them to be moved in an arc near the test section. The foil and glass bottom thermocouples were installed through the back of the vessel near the bottom.

B. NORMAL OPERATION

Initial test runs were made with foils provided with crystals sensitive to two different temperature ranges near the expected foil temperature to determine which crystal would be most appropriate for taking photographs of the boiling phenomenon. Each series of test runs was begun by filling the test vessel with distilled Freon 113 to about 18mm above the surface of the test foil. Both heaters were then energized to bring the system to saturation temperature for measuring zero level and to remove any trapped gasses from the system. The test section power was then secured and the level lowered until the foil surface was even with the liquid surface. The test section was then leveled by adjusting the leveling screws and observing the four corners of the foil to ensure that they were all even with the liquid surface. Zero level was then read and recorded. The vessel was then refilled to about 18mm. Power was then adjusted to the desired level on the test section and on the auxiliary heater to maintain the

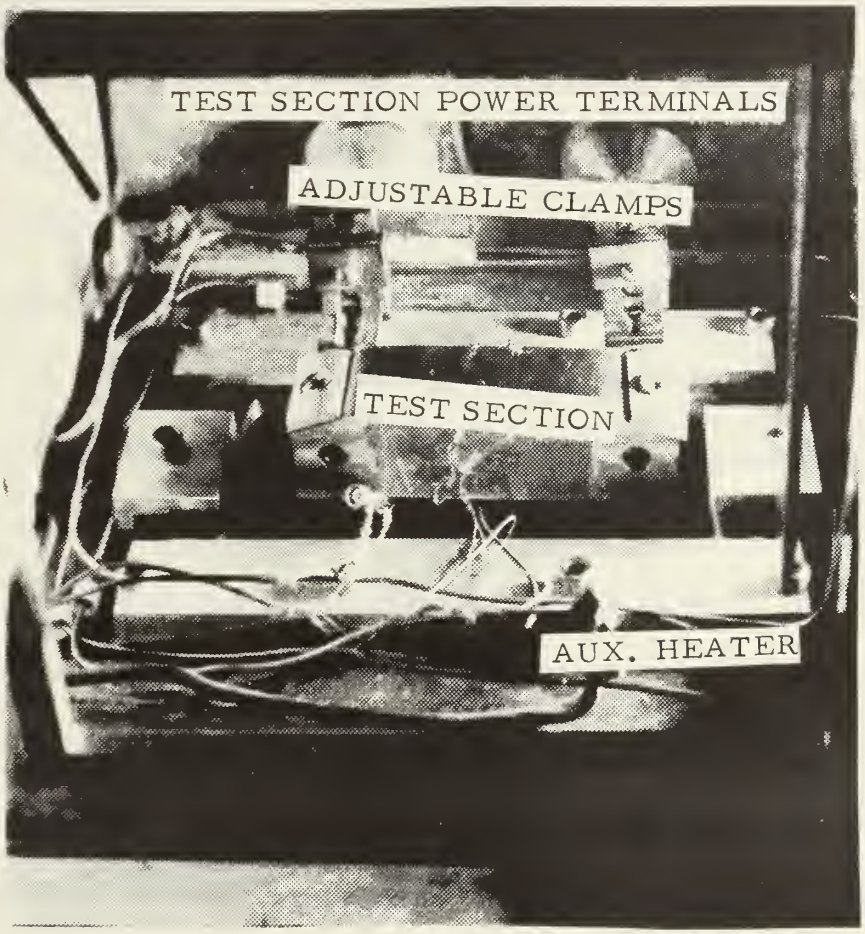

Figure 6.
Test section in place in test vessel
viewed through removable side of test vessel.

system at saturation conditions. Steady state was reached in about 30 minutes. Readings were taken of level, inline voltage, input terminal voltage, all thermocouple outputs, and auxiliary power voltage and current. Liquid level was determined with the micrometer device described in Section II. Auxiliary power readings were taken from the gages on the power supply. All other data was read and recorded by the Hewlett-Packard data acquisition system with each voltage printed out five times. Level was then lowered in increments of about .020 inches (0.5mm) until dryout occurred with the above readings being repeated at each level. During the Group B testing photographs were taken of the crystals and the boiling phenomenon at selected levels. Each test day a reading of barometric pressure was taken to verify saturation temperature of the fluid.

The color photos were taken by turning on the Colortran lights to focus the camera and then turning them off again and allowing the test section to recover from the heating effect of having them on. The heating effect of these lights caused significant distortion of the liquid crystal data, the longer the lights were on the worse the distortion. To minimize this effect during the Group B test runs the lights were turned on just before the camera shutter was tripped and off again immediately afterwards. Each data point was shot two or three times with an f stop of 4.0, 2.8 and/or 3.5. All black and white photos were shot at an f stop of 2.8 using a 100 watt incandescent light with reflector.

C. DATA REDUCTION

The first step in the reduction of the data was to take an arithmetic average of the five numbers recorded for each parameter by the data acquisition system. The thermocouple values were then corrected by adding .006mv, determined from the calibration data, and then converted to degrees centigrade using standard conversion tables. Wall temperature was determined by averaging the readouts from TC Nos. 4 and 5 prior to converting to degrees.

Level was determined by subtracting the zero level reading from each level reading and converting to mm by multiplying by 25.4 mm/inch.

Power to the test section was determined from the following equation

$$PWR = F(S/Rs)$$

where

S - calibrated in-line resistor voltage

F - test assembly input voltage

Rs - inline resistance

The heat flux was determined from:

$$q'' = (PWR - L)/A$$

where

PWR - as determined above

A - test surface area

and L was determined from:

$$L = kA(Tw - T3)/t$$

where

L - heat loss through the glass block

k - thermal conductivity of pyrex glass = 0.02637 watts/cm ^{o}C

t - thickness of the glass block

Tw - wall (foil) temperature

T3 - glass bottom temperature

The heat transfer coefficient was determined from:

$$h = q''/(Tw - Ts)$$

where

h - heat transfer coefficient in watts/m^{2} ^{o}C

Ts - saturation temperature (vapor temperature)

q'' - heat flux in watts/m^{2}.

IV. RESULTS

A. EFFECT OF LEVEL ON HEAT TRANSFER COEFFICIENT

As seen in Figures 7A and B the heat transfer coefficient, h decreases slightly as level is lowered from 18 mm to about 2 mm and then rises as level decreases from 2 mm to 0.2 mm. Below 0.2 mm dryout occurs and the value of h drops sharply. At the lower power level the value of h increased by a factor of about 1.25; while at the higher power level the rise over the minimum value was only by a factor of 1.07. This performance is similar to that noted by Nishikawa [1] for Ethyl-alcohol. The increase noted by both MacKenzie and Nishikawa for water was much larger than this. This increase in h is readily observable from Figure 7B but would not appear to exist in Figure 7A until note is taken of the sparsity of data points between 1.8 and 0.1 mm at the lowest power setting for the Group A data.

From examination of the curves of Figure 7 it would appear that the values of h obtained in the Group A data were about half as great as those for Group B data for nearly the same heat flux. In trying to resolve this discrepancy the test sections for both groups were examined under a microscope since it was noted that the apparent cause arose in a much higher Tw measured in Group A. It was discovered in this examination that the only good thermocouple on test

Figure 7A
Heat Transfer Coefficient
vs
Liquid Level
Group A

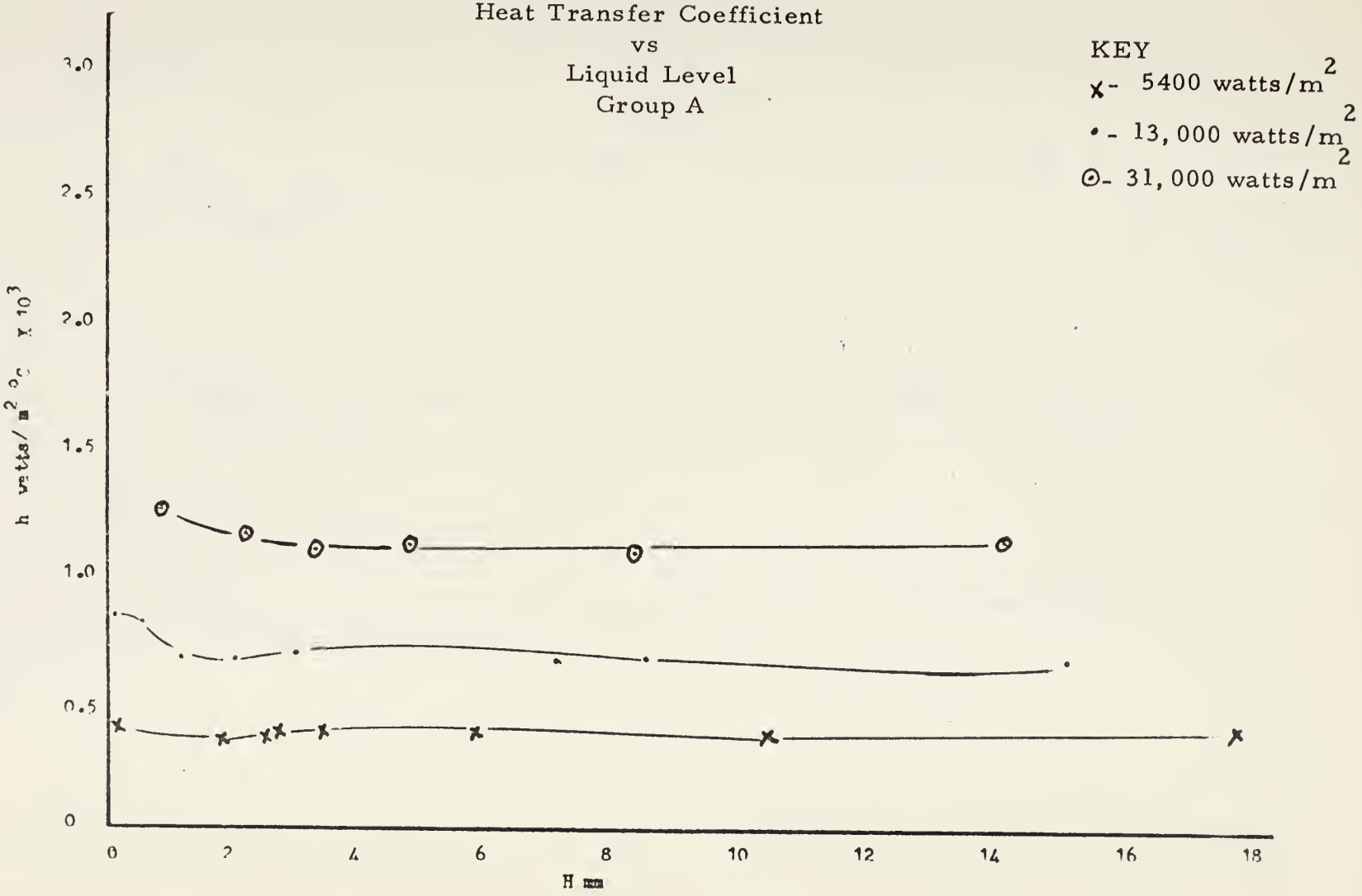

Figure 7B
Heat Transfer Coefficient
vs
Liquid Level
Group B

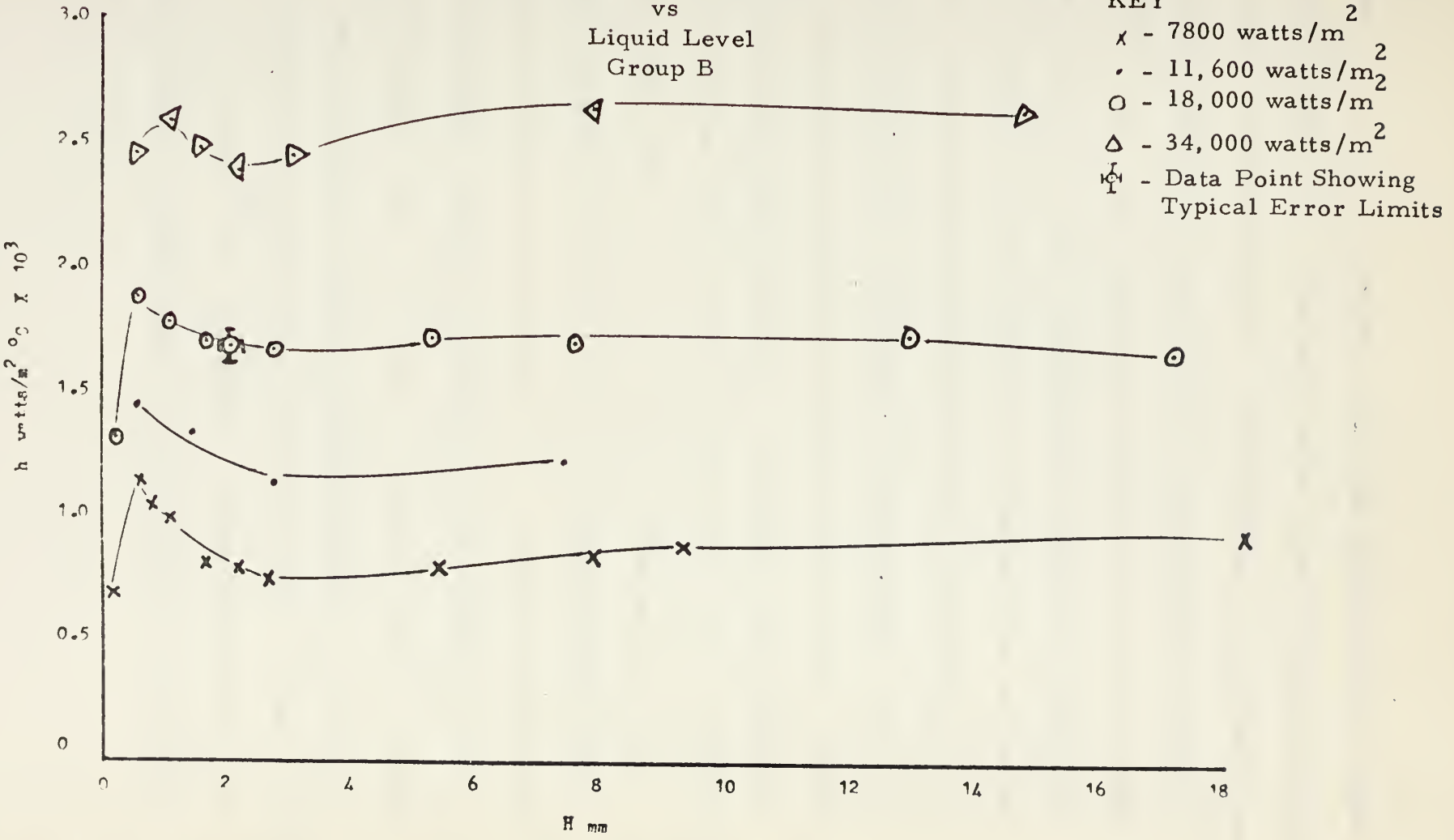

section A was welded so that the wires from the flattened bead came in contact with the edge of the foil at points separated by approximately 0.01 mm as shown in Figure 8. The calculations in Appendix B show that this separation can cause an error in thermocouple read out of .337 millivolts. At the operating temperature of the foil this could result in an error of 7.8°C. To determine if this was actually the source of the error the test section was replaced in the test vessel and the system brought to steady saturation at a nominal power of 40 watts on the test foil. Readings were taken of power, Tw, and T3. The power leads were then reversed and the readings repeated. The data is presented in Appendix B. From this it was determined that the TC on test foil A was being influenced by about 0.9 millivolts at this power setting. This test verified a distortion due to the potential developed by the foil voltage on the thermocouple wires. It indicates an error in Tw of about 20°C. By taking an average of the thermocouple readings to determine Tw, an average Ts, and estimating losses from Group B data, a value for h of 3404.6 watts/$m^{2}{}^{\circ}C$ was calculated. Using the readings obtained with the power leads in the normal position alone and the same loss estimate a value of 11.57.6 watts/$m^{2}{}^{\circ}C$ was calculated. Comparing these with the curves of Figure 7 indicates that this is the source of the error in the Group A data.

Test Section A

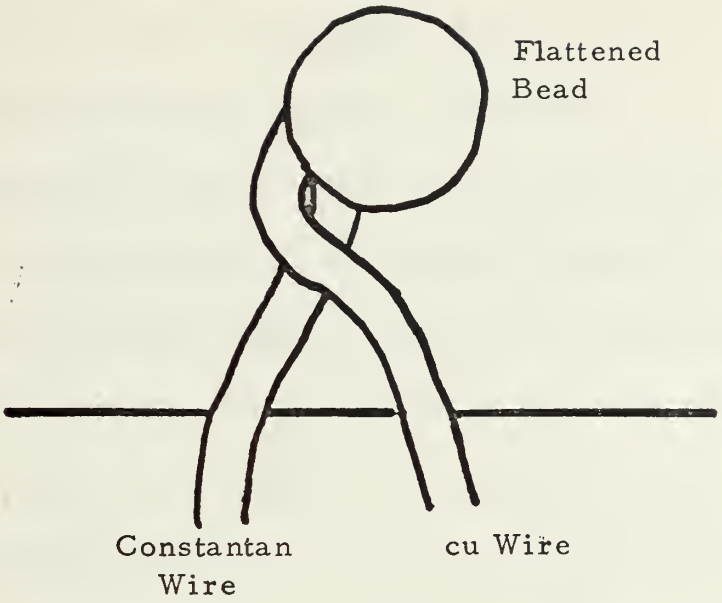

Test Section B

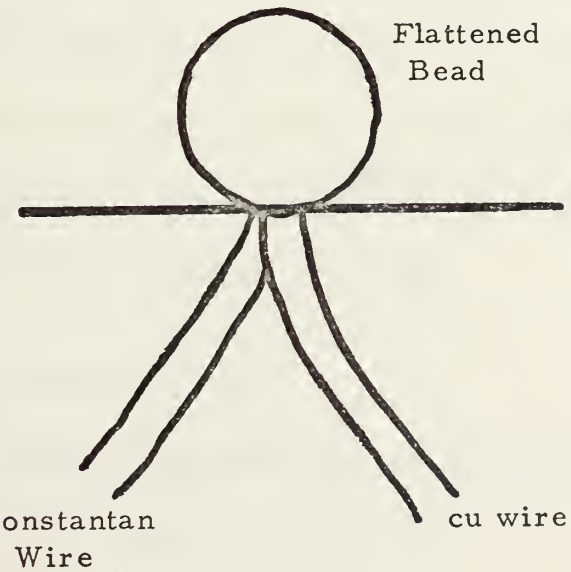

Figure 8
Magnified View of T. C. Attachment to Test Foil

B. CORRELATION OF LIQUID CRYSTAL DATA

Examination of the photographs in Figure 9 confirms the fact that the wall is cooled as liquid level is lowered. This is indicated by the increasing size of the black areas around the perimeter of the foil. At the higher levels the entire foil is above the event temperature of the crystals used. As the level was lowered the cool black spots appeared beneath the nucleation sites on the surface confirming the fact as noted by Raad and Myers that the area beneath the bubbles is a "cold spot" as compared to the "hot spots" under the remainder of the fluid. A direct correlation may be seen by comparing the cooling trend indicated by these photo sequences and the thermocouple data tabulated in Appendix A.

The photographic data obtained in this study does not enable one to determine whether the slight increase in black area observed is due to an increase in the number of nucleation sites or that merely more sites are being cooled into the event temperature range of the crystal used. Comparison of sequence 1 and 2 of Figure 9 does imply that there is an increase in the number of nucleation sites with an increase in heat flux as stated by Nishikawa et al. [2].

C. ABSENCE OF CONVECTION

This study verifies the phenomenon noted by Nishikawa et al. [2] that the bubbles rise straight up rather than in the convection patterns

Figure 9.
Liquid Crystal Photos

A. SEQUENCE AT 7800 watts/m^2

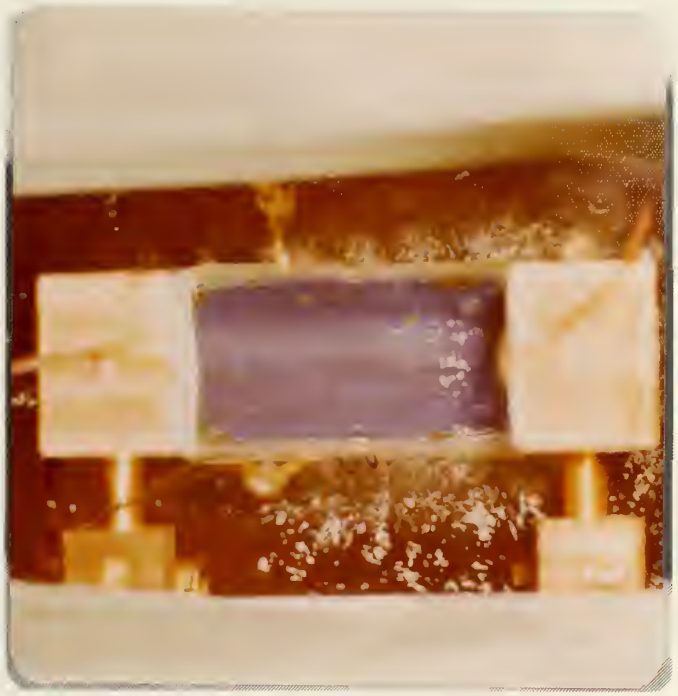

1. H = 2.0 mm

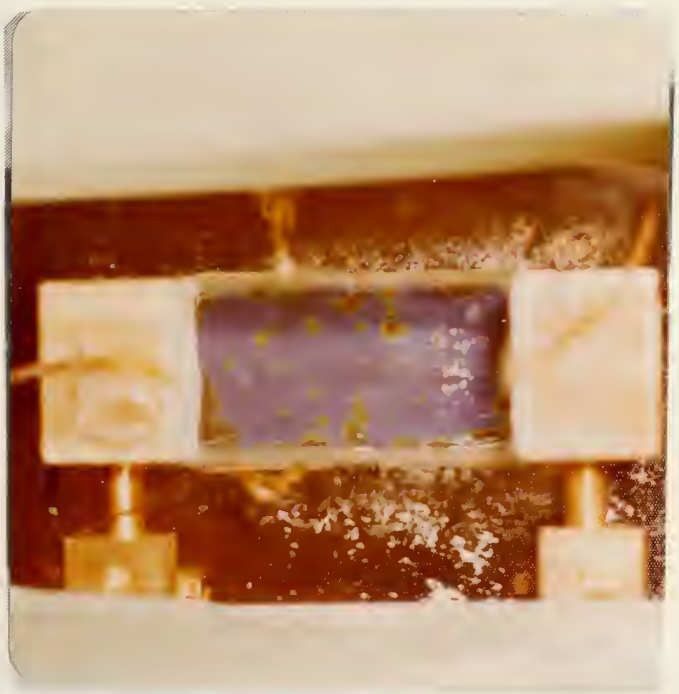

2. H = 1.6 mm

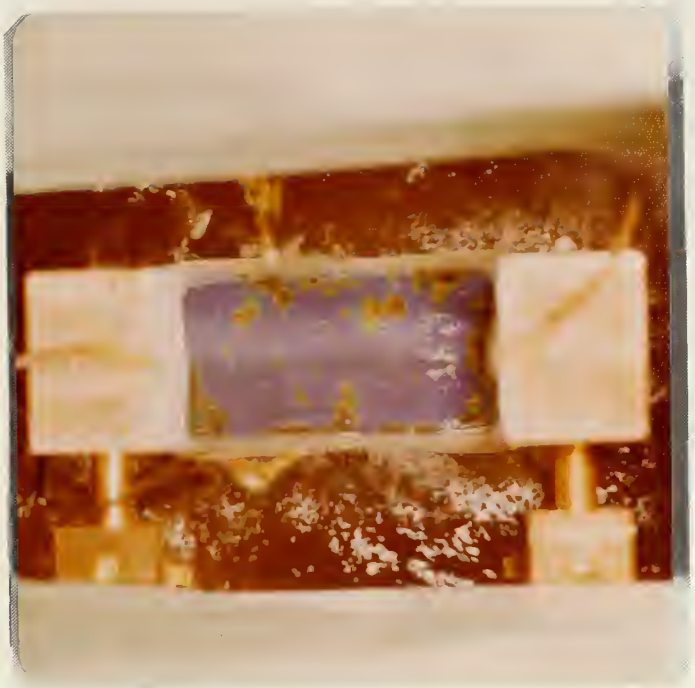

3. H = 1.0 mm

4. H = .5 mm

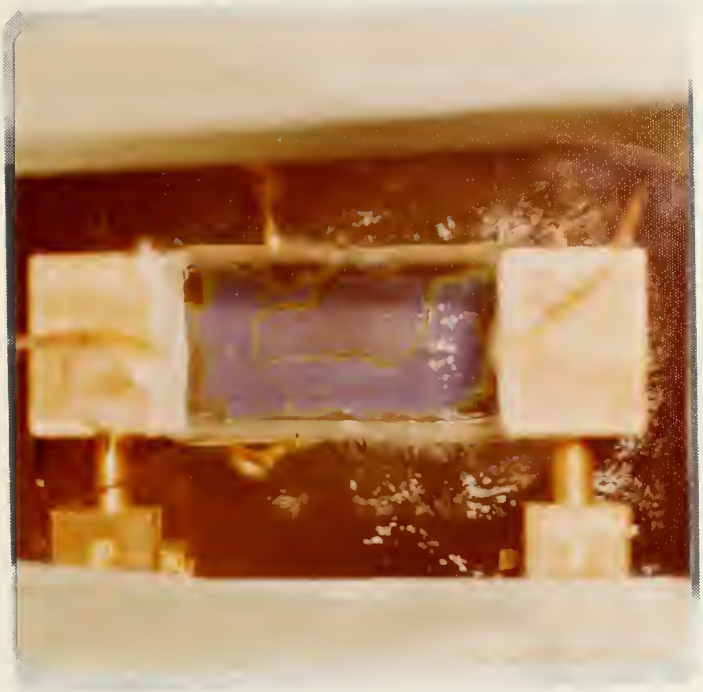

5. H = 0.1 mm

B. SEQUENCE AT 12000 watts/m^2

1. H = 2.7 mm

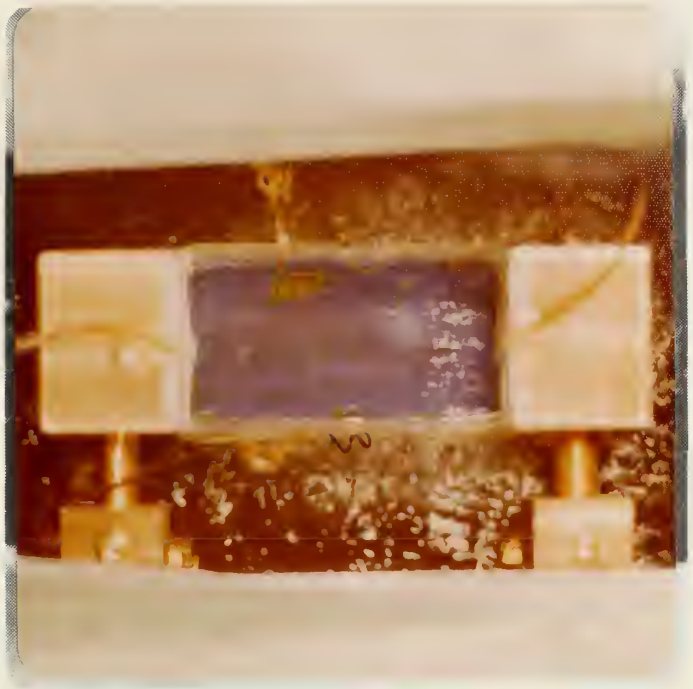

2. H = 1.4 mm

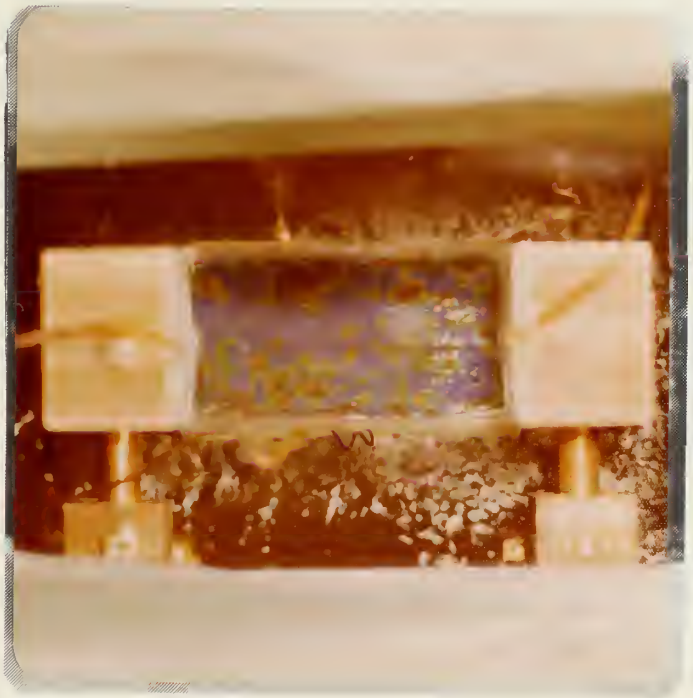

3. H = .5 mm

C. SEQUENCE AT 18,000 watts/m^2

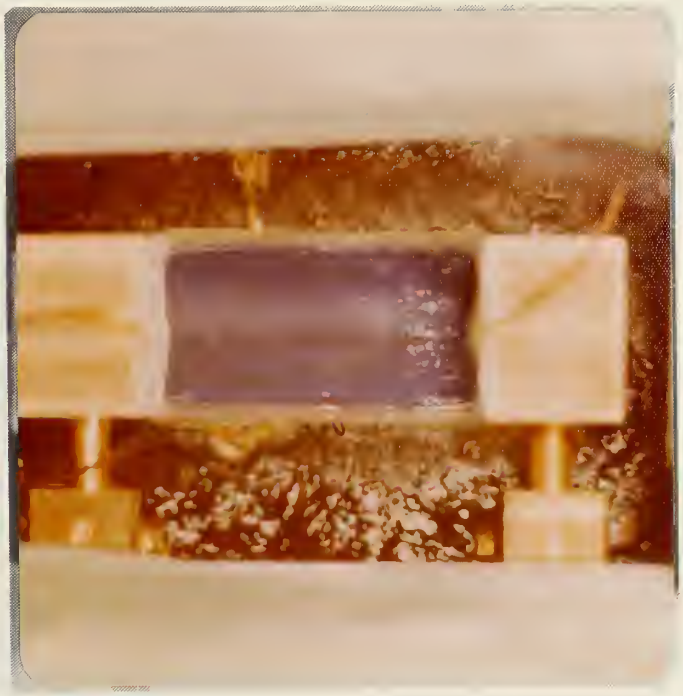

1. H = 2.0 mm

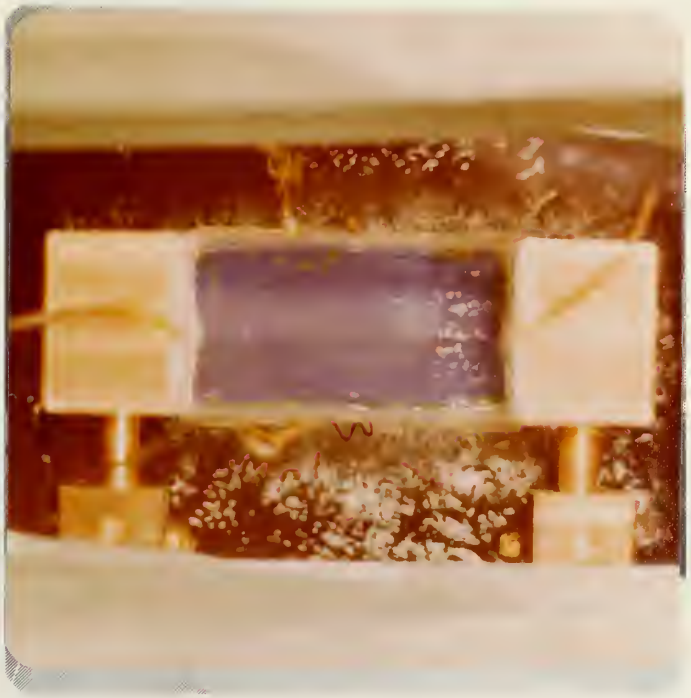

2. H = 1.0 mm

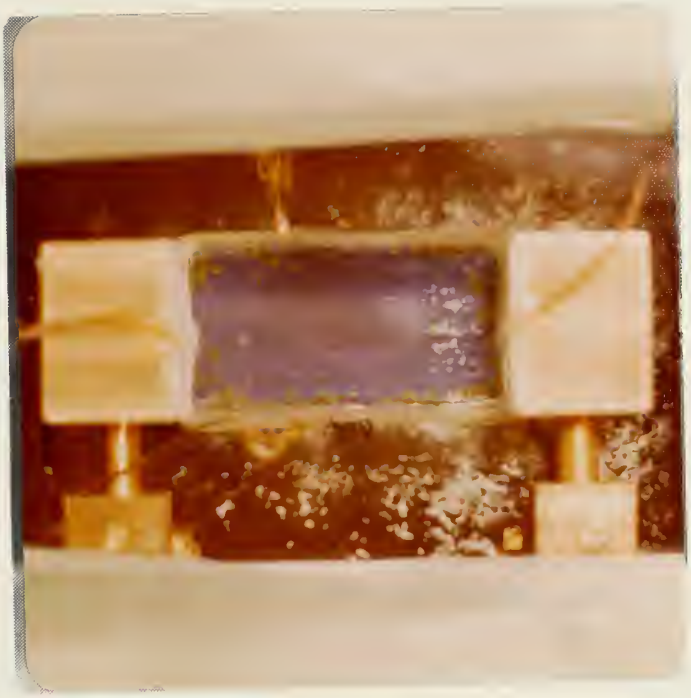

3. H = 0.5 mm

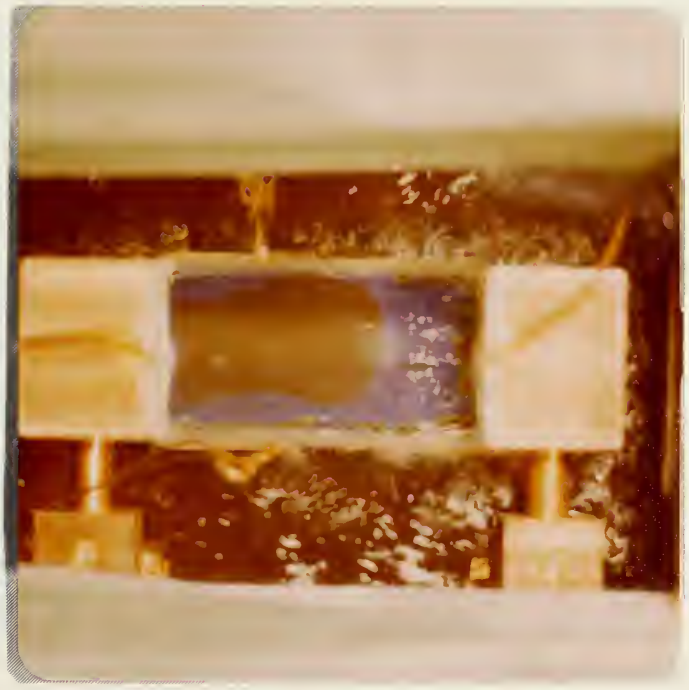

4. H = 0.2 mm

common to pool boiling for the levels below 18 mm studied. The photo of Figure 10 shows the large column of bubbles rising straight up from the test surface. The sparse bubbles around this column originate on the auxiliary heater coil. This phenomenon prevented the convection interference seen in Raad and Myers [4] data.

D. DRYOUT PHENOMENON

Of particular significance is the large irregularly shaped area in Figure 9A5. This photo was shot at a level of 0.1 mm and the area mentioned corresponds to an area experiencing dryout of the test surface. The blue area around this area remained wetted by the Freon 113. The dryout phenomenon is explained by Patten and Turmeau [8] in considerable detail. Evaporation of the thin layer of liquid between the wetted area and the dryout area causes the cool areas on this boundary indicated by the thin green and black boundary seen in Figure 9A5. This phenomenon is similar to the microlayer evaporation presented by Cooper and Lloyd [9]. The dryout observed in this study was that described by Patten and Turmeau as Case 1, without a vapor dome. As can be seen in Figure 11 there exist three heat transfer regions on the heating surface when dryout occurs. In region 1 heat is transferred to the liquid in contact with the surface and to the vapor by evaporation and boiling of this liquid. In region 2 heat is transferred directly to the vapor. In region 3 heat is transferred to the

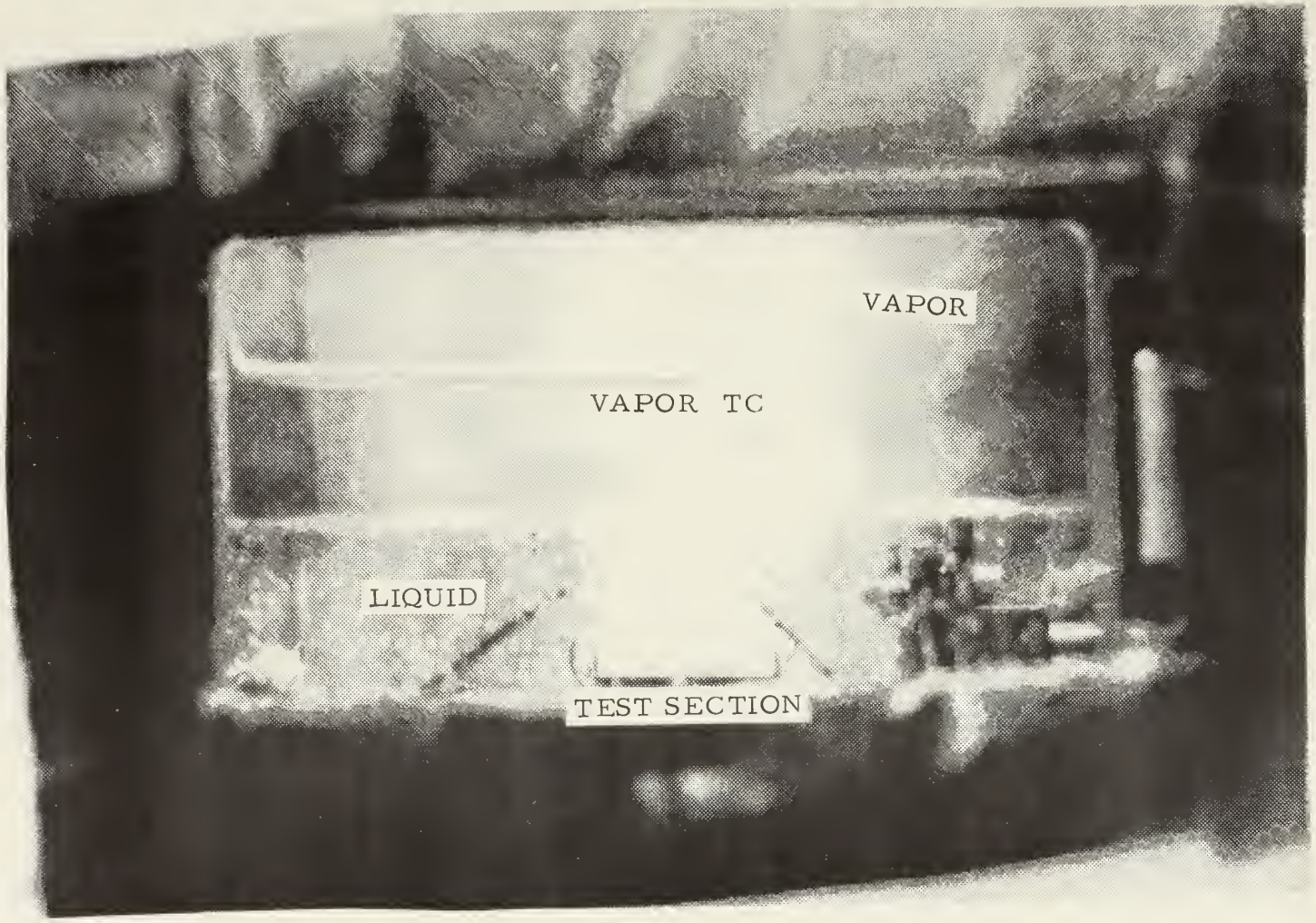

Figure 10.
Test section showing straight bubble rise.

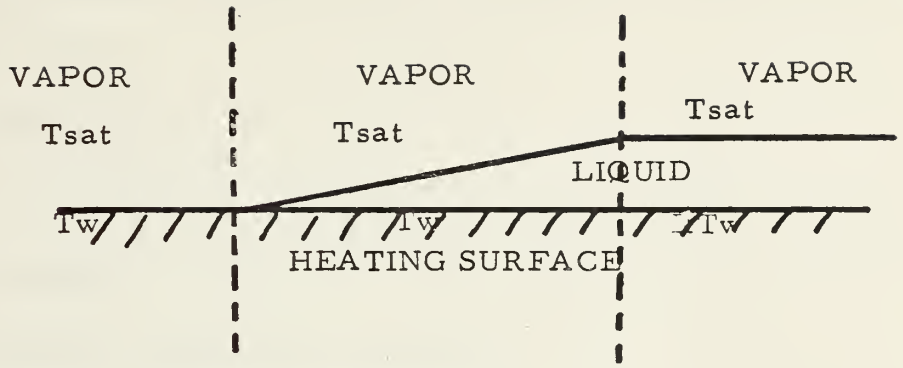

Figure 11.
Dryout Schematic

vapor by evaporation of the thin liquid wedge shaped layer. The mechanism for heat transfer through the liquid layers in both region 1 and 3 for evaporation of the surface is conduction as explained by the following equation;

$$q'' = k(Tw - Ts)/d$$

where

q'' - heat flux

k - thermal conductivity of the liquid

Tw - temperature of heating surface

Ts - saturation temperature of vapor

d - thickness of liquid layer

For a given heat generation rate the quantity q'' is a constant as are k and Ts. For the above relation to hold as d decreases in region 3 the value of Tw must also decrease. Thus heat transfer under a bubble or near the edge of a dryout area is more efficient than with either a continuous liquid layer or a dryout area.

E. PROBLEMS AT HIGH HEAT FLUX

As level was lowered during the runs at 20 and 40 watts in Group B a yellowish liquid residue was observed on the test surface below about 0.8 mm which destroyed much of the data in this region. This residue appeared to have a higher boiling temperature than the Freon 113 being used. The large black area in Figure 9C4 corresponds to the area

covered by this residue. The fact that there is no red or green transition from the blue to black implies several facts, first that there is no dry area between the fluid and the residue, second that the dark area is due to Tw being much greater than the event temperature of the crystals rather than being cooler, which would indicate the third fact, that the residue boils at a higher temperature than the Freon 113. Figure 12 shows schematically how this residue appeared to displace the Freon 113.

At the higher heat fluxes the wall temperature remained above the event temperature of the crystals being used. This fact can be verified by comparing the tabulated wall temperature with the event temperature of the crystals. These event temperatures, obtained from the calibration data presented by Rivers and Field [5], are 56.15°C for the R-56 crystal and 59.15°C for the R- 59 crystal. These temperatures are the green to red transition temperatures during cooling.

F. BOILING PHOTOGRAPHY

Attempts to photograph the boiling action on the test surface through the top window were unsuccessful due to the condensation of large droplets of liquid on the upper viewing window. An attempt to remove these drops by blowing hot air across the window just prior to taking the photos was equally unsuccessful in producing usable

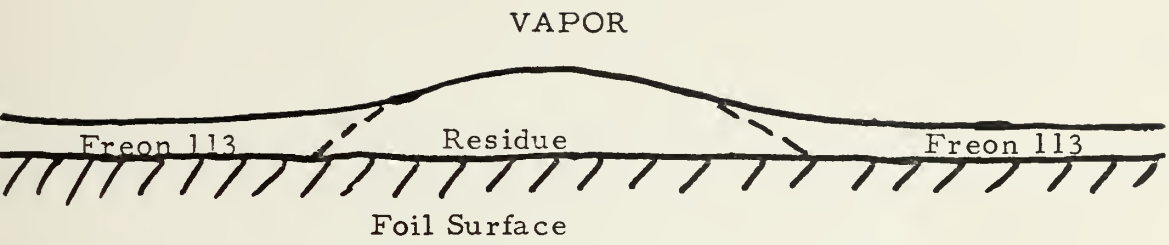

Figure 12.
Schematic of Residue on Foil.
(Note that residue appears to displace
Freon 113 and exist in a thicker layer)

pictures. Thus no correlation between photos of the bubbles on the test surface and the liquid crystal cool spots can be made directly.

V. CONCLUSIONS AND RECOMMENDATIONS

A. CONCLUSIONS

This study has shown that the heat transfer coefficient does indeed increase as liquid level is lowered during boiling in a thin liquid film. This increase is more noticeable at lower heat fluxes.

This study also indicates that liquid crystals are an effective means of mapping nucleation sites during boiling. With some improvements as noted below the author feels that quantitative data may be obtained in this manner.

In Freon 113 bubbles rise straight to the liquid surface from the nucleation sites at liquid levels below 18mm.

The heating surface under the bubbles is cooler than under the undisturbed liquid during boiling.

As heat flux increases the number of active nucleation sites also increases during boiling in thin liquid films.

Wedge-like microlayers around dryout regions cause increased cooling of the heating surface at the boundary between the wetted and unwetted areas.

B. RECOMMENDATIONS

It is highly recommended that this study be continued using a mixture of several crystals as done by Sheppard [6] to map the

nucleation sites at all times rather than only when they are in the range of one crystal.

In further studies using this apparatus it is suggested that several fluids be used to try to avoid the residue problem encountered here. This would also allow greater correlation with the results of other researchers.

An improvement in the technique of applying the foil thermocouples would insure greater confidence in the reproducibility of the results. Great care must be exercised while handling these foils and thermocouples which implies that a better handling jig would be useful.

To insure better photographic results of the boiling phenomena from the top of the vessel it is suggested that a double window similar to the one on the front of the test vessel be installed on the top viewing port. Continuous heating of this window with hot air should prevent the condensation which interfered with the photography of this experiment.

Some form of cold light or electronic flash for illumination of the crystals would significantly improve the quality of the pictoral results.

High speed motion pictures of the color changes of the crystals caused by the boiling action would be a much more efficient method of collecting the data presented by the use of the liquid crystals.

APPENDIX A REDUCED DATA

GROUP A 12 February 1974

Run	Tw °C	Tsat °C	T3 °C	PWR watts	Tw - T3 °C	L watts	q'' watts/m^2	Tw - Tsat °C	h watts/m^2°C	H mm	A-PWR watts
1	60.704	48.023	47.810	7.132	12.894	.680	5,002.	12.681	394.4	17.8	46
2	61.386	47.881	47.623	7.337	13.763	.725	5,126.	13.505	379.4	10.4	46
3	61.068	47.881	47.595	7.226	13.473	.710	5,051.	13.187	383.0	5.8	46
4	60.273	47.976	47.619	7.124	12.654	.667	5,005.	12.297	407.0	3.4	46
5	60.159	47.976	47.690	7.057	12.469	.657	4,961.	12.183	207.2	2.7	46
6	60.454	48.070	47.167	6.956	13.287	.700	4,850.	12.384	391.6	2.5	22
7	59.988	47.381	46.093	6.859	13.895	.732	4,750.	12.607	376.8	2.5	22
8	59.704	46.834	45.628	6.734	14.076	.742	4,646.	12.870	361.0	1.8	22
9	58.116	47.262	45.233	6.654	12.883	.679	4,633.	10.854	426.8	0.1	22
10	66.523	47.524	46.163	17.593	20.360	1.073	12,806.	18.999	674.0	15.1	18.2
11	66.341	47.623	46.372	17.596	19.969	1.052	12,825.	18.718	685.2	8.5	18.2
12	66.545	47.667	46.419	17.630	20.126	1.061	12,844.	18.876	680.4	5.1	18.2
13	65.386	47.881	46.604	17.526	18.781	.990	12,819.	17.505	732.3	3.7	18.2
14	65.295	47.905	46.744	16.808	18.551	.978	12,271.	17.390	705.6	3.0	18.2
15	65.545	47.881	46.791	16.744	18.754	.988	12,214.	17.664	691.5	2.0	18.2
16	65.227	47.976	46.767	16.501	18.460	.973	12,037.	17.251	697.8	1.2	18.2

17	62.909	48.070	46.791	16.673	16.118	.849	12,595.	14.839	848.8	.6	18.2
18	62.591	47.952	49.000	16.848	13.591	.716	12,505.	14.639	885.4	.2	18.2
19	73.395	47.786	47.254	39.076	26.141	1.378	29,223.	25.609	1141.1	14.1	18.2
20	74.578	48.023	47.190	39.678	27.388	1.443	29,640.	26.555	1116.2	8.3	18.2
21	74.511	47.976	47.048	40.709	27.463	1.447	30,436.	26.535	1147.0	4.8	18.2
22	74.956	48.070	46.767	40.594	28.189	1.486	30,316.	26.886	1127.6	3.3	18.2
23	74.378	47.883	46.860	41.143	27.518	1.450	30,770.	26.495	1161.4	2.2	18.2
24	72.778	48.116	46.791	41.472	25.987	1.370	31,087.	24.662	1260.5	.9	18.2

GROUP B 15 February 1974

Run	Tw °C	Tsat °C	T3 °C	PWR watts	Tw - T3 °C	L watts	q'' watts/m^2	Tw - Tsat °C	h watts/m^2°C	H mm	A-PWR watts
1	55.977	47.952	49.232	9.821	6.745	.355	7,338.	8.025	911.4	18.2	37
2	56.209	47.976	49.146	9.644	7.063	.372	7,188.	8.233	873.1	9.2	37
3	56.581	47.976	49.163	9.670	7.418	.391	7,193.	8.605	835.9	7.8	37
4	57.045	48.000	49.279	9.656	7.766	.409	7,168.	9.045	792.5	5.3	37
5	57.591	48.023	49.207	9.654	8.384	.442	7,141.	9.568	746.3	2.6	37
6	57.091	48.000	49.093	9.684	7.998	.421	7,181.	9.091	789.9	2.1	37
7	56.814	48.000	49.140	9.593	7.674	.404	7,123.	8.814	808.1	1.6	37
8	55.233	48.000	48.907	9.602	6.326	.333	7,185.	7.233	993.4	1.0	37
9	54.860	47.976	48.884	9.577	5.976	.315	7,180.	6.884	1043.0	.7	37
10	54.349	48.000	48.884	9.692	5.465	.288	7,290.	6.349	1148.2	.5	37
11	58.246	47.883	48.953	9.659	9.293	.490	7,108.	10.363	685.9	.1	37
29	56.953	47.925	49.512	14.501	7.441	.392	10,937.	9.028	1211.4	7.3	37
30	57.750	48.046	49.419	14.584	8.331	.439	10,965.	9.704	1129.9	2.7	37
31	56.256	48.070	49.326'	14.496	6.930	.365	10,954.	8.186	1338.1	1.4	37
32	55.698	48.023	49.256	14.629	6.442	.339	11,078.	7.675	1443.4	.5	37
33	55.651			14.553							

12	58.256	47.952	49.676	22.263	8.580	.452	16,908.	10.304	1640.9	17.0	37
13	58.046	48.046	49.814	22.831	8.232	.434	17,362.	10.000	1736.2	12.8	37
14	58.326	48.000	50.232	22.981	8.094	.428	17,483.	10.326	1693.1	7.5	37
15.	58.302	48.032	50.023	23.105	8.279	.438	17,571.	10.279	1709.4	5.2	37
16.	58.605	48.000	50.046	23.292	8.559	.452	17,705.	10.605	1669.5	2.7	37
17.	58.512	47.976	49.860	23.257	8.652	.456	17,675.	10.536	1677.6	2.0	37
18	58.442	48.046	50.023	23.099	8.491	.448	17,559.	10.396	1689.0	1.6	37
19	58.140	48.023	49.744	23.463	8.396	.444	17,844.	10.117	1763.8	1.0	37
20	57.614	48.070	49.790	23.263	7.824	.414	17,712.	9.544	1855.8	.5	37
21	61.368	48.070	50.302	23.062	11.066	.584	17,425.	13.298	1310.3	.2	37
22	60.682	47.952	50.163	43.378	10.519	.556	33,195.	12.730	2607.6	14.6	18.2
23	60.795	48.046	50.209	43.711	10.586	.560	33,450.	12.749	2623.7	7.8	18.2
24	61.886	48.163	50.140	43.870	11.746	.620	33,527.	13.723	2443.1	3.0	18.2
25	62.091	48.023	50.186	43.918	11.905	.628	33,558.	14.068	2385.4	2.1	18.2
26	61.659	48.023	50.140	43.833	11.519	.608	33,508.	13.636	2457.3	1.5	18.2
27	61.023	48.023	49.930	43.661	11.093	.586	33,391.	13.000	2568.5	1.0	18.2
28	61.636	48.093	50.232	43.281	11.404	.602	33,084.	13.543	2442.9	.5	18.2

C. CALIBRATED IN-LINE RESISTOR DATA

Manufacturer's stated resistance	3.3333×10^{-4}	ohms
measured resistance	3.46×10^{-4}	ohms
uncertainty	0.13×10^{-4}	ohms

APPENDIX B

POSSIBLE ERROR IN THERMOCOUPLE OUTPUT DUE TO TEST SECTION VOLTAGE

From basic electrical theory:

$$P = I^2R = VI$$

$$V = IR$$

$$\Delta V = \Delta IR + I \Delta R$$

Since I is constant at all points along the foil, $\Delta I = 0$

thus $V = I \Delta R$ and

$$\frac{\Delta V}{V} = \frac{\Delta R}{R} = \frac{\Delta L'}{L'}$$

where L' is the distance along the test section of the foil

Now assume $\Delta L' = 0.05$ mm (.002 inches)

$$\frac{\Delta L'}{L'} = \frac{0.05}{50.4} = .000992$$

therefore

$$\frac{\Delta V}{V} = .000992$$

With 40 watts on the test section F = 1.698 v thus

$$\Delta V = 1.698 \frac{\Delta V}{V} = 1.684 \text{ mv}$$

From conversion tables at operating temperatures

$$\Delta T_w = 39.2^{\circ}C$$

APPENDIX C

SPECIAL TEST DATA AND RESULTS

Parameter	PWR normal	PWR reversed
TC 1	1.943 mv	1.934 mv
TC 4	3.281 mv	1.485 mv
S	9.390 mv	9.390 mv
F	1.698 v	1.698 v
Tw	78.311 ^{o}C	37.00^{o}C
Ts	47.857 ^{o}C	47.643 ^{o}C
Tw - Ts	30.454 ^{o}C	-10.643 ^{o}C
TC 4*	2.384 mv	
Tw*	58.093 ^{o}C	
Ts*	47.738 ^{o}C	
Tw* - Ts*	10.355 ^{o}C	
PWR	46.079 watts	
q''	35255. watts/m^{2}	
h	1157.6 watts/m^{2} ^{o}C	
h*	3404.6 watts/m^{2} ^{o}C	

* refers to the average value between normal and reversed power hookups.

APPENDIX D

UNCERTAINTY ANALYSIS

The uncertainties for the calculations of this study were estimated by applying the method of Kline and McClintock [10] to the relationships given in Section III. C. resulting in equations 1 through 4 below.

1. $$\frac{\Delta PWR}{PWR} = \sqrt{\left(\frac{\Delta S}{S}\right)^2 + \left(\frac{\Delta F}{F}\right)^2 + \left(\frac{\Delta Rs}{Rs}\right)^2}$$

2. $$\frac{\Delta L}{L} = \sqrt{\left(\frac{\Delta k}{k}\right)^2 + \left(\frac{\Delta t}{t}\right)^2 + \left(\frac{\Delta Tw}{Tw - T3}\right)^2 + \left(\frac{\Delta T3}{Tw - T3}\right)^2 + \left(\frac{\Delta A}{A}\right)^2}$$

3. $$\frac{\Delta q''}{q''} = \sqrt{\left(\frac{\Delta PWR}{PWR - L}\right)^2 + \left(\frac{\Delta L}{PWR - L}\right)^2 + \left(\frac{\Delta A}{A}\right)^2}$$

4. $$\frac{\Delta h}{h} = \sqrt{\left(\frac{\Delta q''}{q''}\right)^2 + \left(\frac{\Delta Tw}{Tw - Ts}\right)^2 + \left(\frac{\Delta Ts}{Tw - Ts}\right)^2}$$

Using data from Appendix A Group B run 17 and the following uncertainty estimates in equations 1 - 4 a representative uncertainty on h was determined and plotted on Figure 7B.

Parameter	uncertainty
S	$\pm$ 2.5 v
F	$\pm$ .48 m v
Rs	$\pm$ 13. ohms
t	$\pm$ 0.1 mm
k	0 - assumed
A	$\pm$ 0.1 cm^2
Tw	$\pm$ 0.12 ^oC
T3	$\pm$ 0.02 ^oC
Ts	$\pm$ 0.02 ^oC

The results of these calculations follow

$$\frac{\Delta PWR}{PWR} = 0.0366$$

$$\frac{\Delta L}{L} = 0.0083$$

$$\frac{\Delta q''}{q''} = 0.0383$$

$$\frac{\Delta h}{h} = 0.039$$

Using this value of $\Delta h/h$ and the value of h from Appendix A, Group B, run 17 of 1677.6 watts/ m^2 ^oC the representative uncertainty in h was found to be $\pm$ 65.4 watts/m^2 ^oC.

The uncertainty in H was estimated to be $\pm$ 0.1 mm.

LIST OF REFERENCES

1. MacKenzie, D. K., Vaporization of Thin Liquid Films, M.A. Thesis, Naval Postgraduate School, Monterey, 1972.

2. Nishikawa, K., Kusuda, H., Yamasaki, K., Tanaka, K., "Nucleate Boiling at Low Liquid Levels," Trans. Japan Society of Mechanical Engineers, V. 10, No. 38, p. 328-338, 1967.

3. Grigor'ev, V. A. and Dudkevich, A. S., "Boiling Cryogenic Liquid in a Thin Film," Teploenerfetika, v. 17, No. 12, p. 54-57, 1970.

4. Raad, T. and Myers, J. E., "Nucleation Studies in Pool Boiling on Thin Plates Using Liquid Crystals," American Institute of Chemical Engineers Journal, v. 17, No. 5, p. 1260-1261, 1971.

5. Rivers, A. D. and Field, R. J., Mapping of Surface Temperatures with Cholesteric Liquid Crystals, 3430 Report, Naval Postgraduate School, Monterey, 1973.

6. Sheppard, F., Liquid Crystal Mapping of the Surface Temperature on Electronic Circuit Boards, 3430 Report, Naval Postgraduate School, Monterey, 1973.

7. Naval Underwater Sound Center Technical Report 4235, Utilization of Temperature Sensitive Liquid Crystals for Thermal Analysis and an Application to Transducer Investigations, by R. D. Maple, 1972.

8. Patten, T. D. and Turmeau, W. A., "Some Characteristics of Nucleate Boiling in Thin Liquid Layers," Heat Transfer 1970, v. V, Paper No. B 2.10, 1970.

9. Cooper, M. G. and Lloyd, A. J. P., "The Microlayer in Nucleate Pool Boiling," Int. Journal of Heat and Mass Transfer, v. 12, p. 895-913, 1969.

10. Kline, S. J. and McClintock, F. A., "Describing Uncertainties in Single-Sample Experiments," Mechanical Engineering, v. 75, p. 3-8, January 1953.

INITIAL DISTRIBUTION LIST

		No. Copies
1.	Defense Documentation Center Cameron Station Alexandria, Virginia 22314	2
2.	Library, Code 0212 Naval Postgraduate School Monterey, California 93940	2
3.	Department Chairman, Code 59 Department of Mechanical Engineering Naval Postgraduate School Monterey, California 93940	2
4.	Professor Paul J. Marto (Code 59Mx) Department of Mechanical Engineering Naval Postgraduate School Monterey, California 93940	1
5.	LT Almon D. Rivers, USN c/o COMCRUDESPAC (Code 316) San Diego, California 92132	1

150814
Thesis
R586
c.1
Rivers
An experimental investigation of nucleate boiling in thin liquid films.